

Articles

Design and Synthesis of Potent Inhibitors of the Malaria Parasite Dihydroorotate Dehydrogenase

Timo Heikkilä,[†] Christopher Ramsey,[†] Matthew Davies,[†] Christophe Galtier,[‡] Andrew M. W. Stead,[†] A. Peter Johnson,^{*,†} Colin W. G. Fishwick,^{*,†} Andrew N. Boa,^{*,‡} and Glenn A. McConkey^{*,†}

School of Chemistry and the Astbury Centre for Structural Molecular Biology, and Faculty of Biological Sciences, University of Leeds, Leeds LS2 9JT, UK, and Department of Chemistry, University of Hull, Cottingham Road, Hull HU6 7RX, UK

Received June 8, 2006

Pyrimidine biosynthesis presents an attractive drug target in malaria parasites due to the absence of a pyrimidine salvage pathway. A set of compounds designed to inhibit the *Plasmodium falciparum* pyrimidine biosynthetic enzyme dihydroorotate dehydrogenase (PfDHODH) was synthesized. PfDHODH-specific inhibitors with low nanomolar binding affinities were identified that bind in the N-terminal hydrophobic channel of dihydroorotate dehydrogenase, the presumed site of ubiquinone binding during oxidation of dihydroorotate to orotate. These compounds also prevented growth of cultured parasites at low micromolar concentrations. Models that suggest the mode of inhibitor binding is based on shape complementarity, matching hydrophobic regions of inhibitor and enzyme, and interaction of inhibitors with amino acid residues F188, H185, and R265 are supported by mutagenesis data. These results further highlight PfDHODH as a promising new target for chemotherapeutic intervention in prevention of malaria and provide better understanding of the factors that determine specificity over human dihydroorotate dehydrogenase.

Introduction

Nucleic acid synthesis in species of *Plasmodium* differs from most organisms by the complete reliance on purine salvage due to the absence of de novo purine synthesis and, conversely, the absence of salvage of pyrimidine nucleobases and nucleosides. Genes encoding enzymes for purine ring synthesis are not identifiable in the *Plasmodium falciparum* genome. In contrast, genes encoding the eight enzymes in de novo pyrimidine synthesis have been identified.¹ The dependence of *Plasmodium* on pyrimidine biosynthesis renders the pathway a valid target for development of novel antimalarial drugs.^{2,3} Dihydroorotate dehydrogenase (DHODH) catalyzes the oxidation of the intermediate dihydroorotate to orotate. The type 2 DHODHs, found in Gram-negative bacteria and eukaryotes, catalyze the reaction by a two-site “ping-pong” mechanism with flavin mononucleotide (FMN) serving as an intermediate in the electron transfer and ubiquinone acting as the final electron acceptor. The type 2 DHODHs feature a conserved α/β barrel core structure, which contains the catalytic site that binds substrate dihydroorotate and FMN, and an N-terminal hydrophobic domain as shown by the crystal structures of *Escherichia coli*, human, rat, and, most recently, *P. falciparum* DHODH.^{4–7} The N-terminal domain is thought to be the site of ubiquinone binding and is the site of action of a number of DHODH inhibitors.

DHODH is an established target for antibiotics and treatment for autoimmune diseases. The potent human DHODH inhibitor

leflunomide (Arava) is in clinical use [the active metabolite is **1** (A77 1726) in Figure 1] for treatment of rheumatoid arthritis.^{8,9} Inhibitors of *Helicobacter pylori* DHODH and *Enterococcus faecalis* DHODH have been described that inhibit bacterial growth.^{10,11} *P. falciparum* DHODH (PfDHODH^o) is also an attractive target for drug development, since disrupting PfDHODH activity using inhibitors or lowering the expression levels of PfDHODH inhibits parasite growth.^{12–14} PfDHODH has been localized to the inner mitochondrial membrane in blood stage parasites.¹² Interestingly, the antimalarial drug atovaquone, an ubiquinone mimic, is thought to disrupt the transfer of electrons at cytochrome BC1, and parasites treated with atovaquone have reduced levels of orotate.^{15,16} Cocrystal structures of human, rat, and *P. falciparum* DHODH show that A77 1726 and atovaquone bind within the putative ubiquinone binding channel.^{5–7} Therefore, this channel is the logical target for development of new chemotherapeutics against PfDHODH and has already been used for structure-based drug design applications.¹⁷ It has also been found to be the binding site of novel inhibitors identified from a high-throughput screen (**2** and **3**, Figure 1).¹⁸ In this study, we report a new class of PfDHODH-specific inhibitors with high binding affinities and analyze the mode of binding through modeling and mutagenesis.

Results and Discussion

Chemistry. The tetracyclic compound **4** (3,4-dimethyl-1,5-dihydropyrrolo[3,2-*b*]carbazole-2-carboxylic acid ethyl ester) was originally prepared by Shannon and found to inhibit cell growth in a similar fashion to **1** and brequinar.¹⁹ As part of a

* Corresponding authors. G.A.M.: phone, +44 113 3432908; fax, +44 113 3432835; e-mail, g.a.mcconkey@leeds.ac.uk. A.N.B.: phone, +44 1482 465022; fax, +44 1482 466410; e-mail, a.n.boa@hull.ac.uk. A.P.J.: phone, +44 113 3436515; fax, +44 113 3436530; e-mail, a.p.johnson@leeds.ac.uk. C.W.G.F.: phone, +44 113 3436510; fax, +44 113 343653; e-mail, c.w.g.fishwick@leeds.ac.uk.

[†] University of Leeds.

[‡] University of Hull.

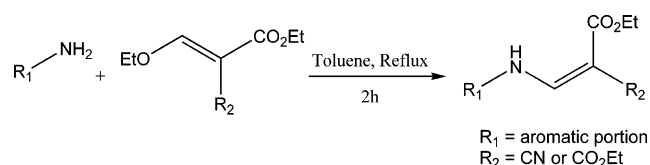
^o Abbreviations: PfDHODH, *Plasmodium falciparum* dihydroorotate dehydrogenase; HsDHODH, human dihydroorotate dehydrogenase; DCIP, 2,6-dichloroindophenol; DHO, dihydroorotate; CoQ, ubiquinone coenzyme, CoQ_D, decylubiquinone.

Compound ID	Structure
1	
2	
3	
4	

Figure 1. A77 1726 (**1**), two of the most potent PfDHODH inhibitors identified in a high-throughput screen by Baldwin et al.¹⁸ (**2** and **3**), and the lead compound (**4**).

larger program, where analogues of inhibitors of human DHODH are being evaluated against PfDHODH,²⁰ we set out to resynthesize this derivative and subsequently found it to have modest activity against PfDHODH. However, the preparation of this heterocycle is not straightforward using Shannon's method and, as we required access to a range of similar derivatives, we envisioned a general strategy starting from the 3-aminocarbazole nucleus. During this work the derivative **6** (Figure 2) was prepared by simple condensation between *N*-ethyl 3-aminocarbazole and ethyl 3-ethoxy-2-cyanoacrylate. Com-

Scheme 1



ound **6** was prepared with the intention of subsequent cyclization to a pyridocarbazole. However, during a routine screen it was found to be quite active against PfDHODH. Following this discovery, a set of compounds based loosely on this lead structure was synthesized from a range of commercially available monocyclic, bicyclic, or tricyclic aromatic amines. In the case of compounds **11**–**14**, the biphenyl amines were obtained by Suzuki cross-coupling of the appropriate bromoaniline and benzenboronic acid in the presence of palladium acetate and triphenylphosphine. The amines were coupled with diethyl ethoxymethylenemalonate or ethyl 3-ethoxy-2-cyanoacrylate by simply stirring in refluxing toluene for 2 h (Scheme 1) to produce a set of analogues containing common "head" groups but with variations in the aromatic portion of the molecule.

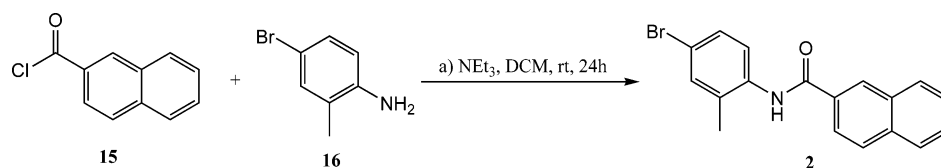
Compounds **2** and **3**, previously identified as potent inhibitors of PfDHODH,¹⁸ were also synthesized as reference compounds. Compound **2** was obtained in 49% yield from commercially available **15** (2-naphthoyl chloride) and **16** (4-bromo-2-methylaniline) (Scheme 2). Compound **3** was synthesized from **17** (2-methyl-3-nitrobenzoic acid) in 52% yield by conversion to **18** (2-methyl-3-nitrobenzoyl chloride) and subsequent treatment with **19** (3,5-dichloroaniline; Scheme 3).

Biological Data and Structure–Activity Relationships. The compounds were tested against a recombinant PfDHODH expressed from a synthetic gene in which codon usage has been optimized for expression in *E. coli*. From the initial screening of 17 synthesized compounds, six (**5**–**10**; Figure 2) inhibited PfDHODH activity with detectable levels (>10% at 10 μM).

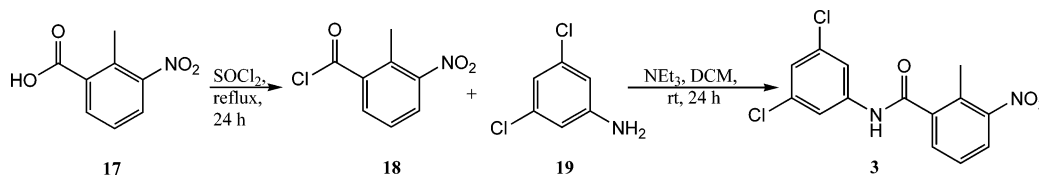
Compound ID	Structure	Compound ID	Structure
5		10	
6		11	
7		12	
8		13	
9		14	

Figure 2. List of the compounds that were found to inhibit PfDHODH.

Scheme 2



Scheme 3

**Table 1.** Activity of Compounds against *P. falciparum* and Human DHODH

inhibitor	PfDHODH		HsDHODH		selectivity (fold)
	IC ₅₀ (μM) (SE)	K _i (μM)	IC ₅₀ (μM)	K _i (μM)	
5	0.16 ± 0.05	0.02	29.57 ± 5.9	3.63	182
6	0.44 ± 0.06	0.05	491.4 ± 42.4	60.40	1208
7	27.78 ± 3.2	3.20	123.3 ± 26.3	15.10	5
8	40.00 ± 5.2	4.60	145.7 ± 31.2	17.90	4
9	345.6 ± 29.4	39.70	292.2 ± 41.6	35.90	1
10	349.1 ± 26.4	40.20	>500	na ^a	na
11	>500	na	>500	na	na
12	>500	na	>500	na	na
13	21.3 ± 8.2	2.45	219.8 ± 33.2	27.0	10
14	86.7 ± 11.2	10.0	104.2 ± 21.3	12.8	1
2 /no. ^{2b}	0.18 ± 0.09	0.02	415.4 ± 53.5	50.9	2308
3 /no. ^{6b}	0.23 ± 0.12	0.03	524.4 ± 43.5	64.4	2280
1/A77 1726	190.1 ± 10.32	23.35	0.26 ± 0.10	0.03	0.001

^a na = not applicable. ^b high-throughput screening compounds from Baldwin et al.¹⁸

The six compounds all contain a polar “head group” linked through a nitrogen to an aromatic or heteroaromatic moiety. We noted immediately the similarity between these structures, most notably **8** and **1**, which both contain an amino aromatic unit with a polar substituent of roughly similar functionality and dimensions. The six compounds exhibited a range of apparent inhibition coefficients (K_i^{app}) between 20 nM and 40 μM. Five of the six active compounds (**5**, **7–10**) have a methylenemalonate group, and interestingly, the tricyclic compounds (**5** and **6**) are more active than the monocyclic or bicyclic compounds. To determine the specificity for PfDHODH, the affinity of these inhibitors was also measured for HsDHODH. The compounds had considerably lower affinity for the human enzyme, showing up to 1200-fold higher relative affinity for the parasite enzyme. Furthermore, the biphenyl analogues of compounds **5** and **6** (**11** and **12**) displayed reduced activity in both enzymes (IC₅₀ > 500 μM). The *m*-biphenyl structures **13** and **14** displayed activity at low micromolar concentrations but with loss of selectivity, with respect to compounds **5** and **6**.

A series of simple aromatic amide-based inhibitors of PfDHODH has also recently been identified through a high-throughput screening approach.¹⁸ In parallel assays, we find that **5** and **6** bind PfDHODH with similar affinity to the two most active compounds reported in the previous study (**2** and **3**; Table 1).

It is noteworthy that although a truncated enzyme was used in both studies, the expressed enzyme in our assay contained additional N-terminal amino acids derived from the native protein (F158–Y169). In the X-ray crystal structure of PfDHODH, these residues have a well-defined structure, forming the entrance and partially lining the hydrophobic ubiquinone

binding channel by making up half of the first N-terminal α-helix.⁷ Additionally, residues E164 and E182 form a salt bridge that seems to anchor the N-terminal helix to the α/β barrel as also seen in the HsDHODH structure.^{5,7} The use in the previous study of a truncated enzyme that does not include these N-terminal residues may explain the differences in the measured affinities observed in the two studies.

Competition analysis supports binding of inhibitors in the N-terminal hydrophobic channel of PfDHODH. The Michaelis constants, K_M , for DHO and the synthetic ubiquinone CoQ_D measured in our assays were 31.4 ± 2.8 and 13.4 ± 0.8 μM, respectively, in agreement with published values.¹⁴ In experiments varying CoQ_D concentrations in the presence of set concentrations of **5** there was an increase in apparent K_M but unchanged v_{max} , consistent with competitive inhibition of binding of CoQ_D (Figure 3A). Analysis of competition with CoQ_D via global fitting of the data set found the best fit with curves generated using the equation for competitive inhibition (goodness of fit R^2 of 0.92). It was not possible to fit a curve that converges to the data using the equation for noncompetitive inhibition. The results of nonlinear regression using the equation for uncompetitive inhibition were extremely discordant with Lineweaver–Burk analysis. Hence, competition with CoQ for binding was supported as has been found with most other DHODH inhibitors.^{18,21,22} In contrast, varying DHO concentration with set concentrations of **5** and saturating CoQ_D exhibited no change in K_M and a decrease in v_{max} of PfDHODH, indicating uncompetitive inhibition (Figure 3B). These data strongly support the ligand binding site being within the hydrophobic ubiquinone channel. In structures of mammalian DHODH and PfDHODH cocrystallized with ligands, the ligands bind within the hydrophobic channel between two α-helices at the N-terminus of DHODH. This binding appears to impair the ability of ubiquinone to diffuse into the enzyme during catalysis to reoxidize FMN.

Importantly, compounds **5** and **6** were also found to be active against cultured malaria parasites with IC₅₀ of 1.8 ± 1.1 and 4.0 ± 1.2 μM, respectively. These results further emphasize the potential for using DHODH as a target for developing antimalarials.

Modeling the Binding of Inhibitors 5 and 6. Structural binding models of compounds **5** and **6** were constructed using the X-ray crystal coordinates of PfDHODH in complex with DHO and A77 1726 (PDB ID 1TV5). Two different docking systems, Autodock 3.0²³ in combination with the graphical user interface Autodock Tools and eHITS,²⁴ were used for docking **5** and **6** into DHODH structures with DHO and A77 1726 removed. Using precalculated grids of affinity potentials, Autodock evaluated suitable ligand positions on DHODH

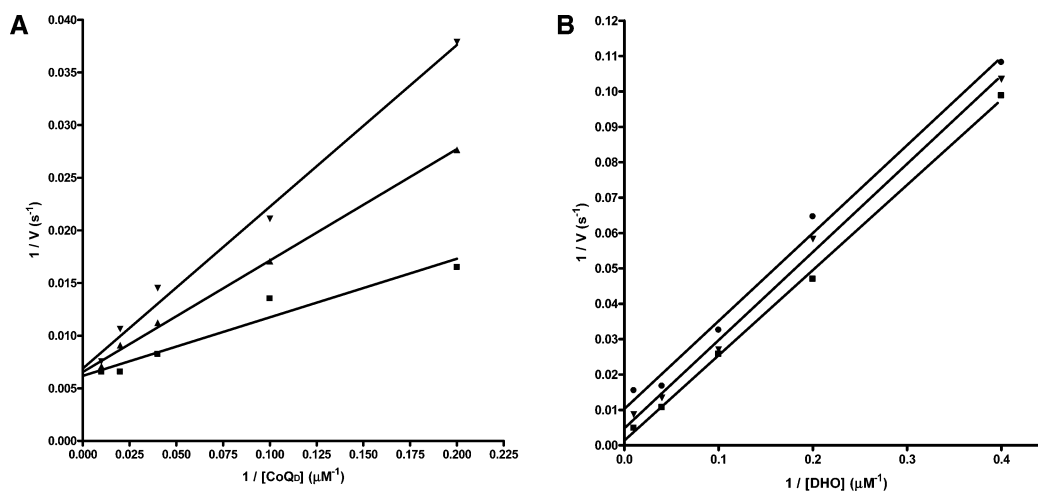


Figure 3. (A and B) Double-reciprocal plots of enzymatic rate as a function of substrate concentration. Substrates coenzyme CoQ_D (A) and dihydroorotate (B) were varied in steady-state kinetic assays. The rates were measured in the absence of inhibitor (■) and with 0.25 μM (▲) and 0.50 μM (▼) of compound **5**. Convergent lines (A) indicate competition of CoQ_D by compound **5**, whereas parallel lines (B) indicate uncompetitive inhibition of DHO.



Figure 4. Models obtained from automated docking of **5** (A) and **6** (B) to PfDHODH. The predicted hydrogen bonds between the inhibitor and amino acid residues are shown as green dashed lines. Also highlighted is the *Plasmodium*-specific F188. Figures were generated with Pymol.

allowing random movements of the ligand conformations on the surface. Free-energy scores were calculated on the basis of a linear regression analysis, the AMBER force field, and the results of training on a large set of diverse protein–ligand complexes with known inhibition constants that are incorporated in the program. The predicted binding affinity was also calculated using the ligand scoring function in the HIPPO module from the de novo molecular design software SPROUT.²⁵ Here, each of the individual best-docked ligand structures was used as the cavity file, and a 6-Å layer of protein centered on this structure was used as the receptor file.

The docked poses with the lowest energies suggest that both these high affinity compounds bind in the hydrophobic channel (Figure 4A,B). Each inhibitor is predicted to make hydrogen-bonding contacts with conserved amino acid residues (residues H185, R265, and Y528) as well as gaining a significant binding contribution from hydrophobic interactions due to the continuous nature of the hydrophobic cavity.

The role of hydrophobicity upon the measured affinities of compounds **5**–**10** for PfDHODH is underlined by their relatively high calculated log *P* values (data not shown).²⁶ Modeling of the binding of **5** in HsDHODH indicates that the side chain of the conserved histidine (H56 in HsDHODH and H185 in PfDHODH, respectively) is locked in a conformation that prevents formation of the hydrogen bond observed in PfDHODH. Furthermore, the surface complementarity is not as good as it is for PfDHODH. The tricyclic hydrophobic moiety fits very well into the hydrophobic pocket of the N-terminal channel in PfDHODH, and the binding model indicates a staggered stacking interaction with F188, whereas in HsDHODH the

Table 2. Kinetics of the Mutant PfDHODH

PfDHODH	kinetic constants for PfDHODH		
	K_m^{app} (M)		k_{cat} (s ⁻¹)
	CoQD	DHO	
wild type	13 ± 1	31 ± 3	15.8 ± 2
H185A	19 ± 1	33 ± 3	1.4 ± 2.3
F188A	17 ± 1	35 ± 2	12.3 ± 4
R265K	13 ± 1	33 ± 4	16.1 ± 5

corresponding residue is A59. The difference in activity between carbazoles **5** and **6** and the biphenyl analogues **11**–**14** suggests an important hydrophobic requirement for selectivity such that the planar carbazole moiety is preferred in PfDHODH. In particular, the *m*-biphenyls **13** and **14**, which only differ from **6** and **5** by lack of the N- and S-links, respectively, are less active and less selective than **6** and **5**, perhaps indicating a nonplanar arrangement between the aromatic rings that does not satisfy the hydrophobic binding region as efficiently. Figure 4 shows the binding model of compounds **5** and **6**, with the planar carbazole moiety stacked against residue F188. A nonplanar biphenyl would clearly lack this favorable hydrophobic stacking interaction.

Analysis of Protein–Inhibitor Interactions by Mutagenesis. The predicted H-bonding and hydrophobic interactions of **5** and **6** with the amino acid residues were tested by generating point mutants of residues H185, F188, and R265 (Tables 2 and 3; The Y528F mutant could not be tested due to the low catalytic activity of the enzyme) of the PfDHODH. Substitutions of these residues led to considerable changes in the binding affinities of

Table 3. Effect of Mutations in PfDHODH on Inhibitor Activity^a

inhibitor	IC ₅₀ against PfDHODH (M)			
	wild type	H185A	F188A	R265K
5	0.16 ± 0.04	124 ± 10	82 ± 6	5.4 ± 0.8
6	0.44 ± 0.08	128 ± 8	70 ± 6	32 ± 5

the inhibitors without dramatically affecting the substrate binding affinities. Hence, consistent with our modeling predictions, these residues are involved in binding **5** and **6**, although other interactions are likely to contribute. Interestingly, the unique conformation observed for the conserved histidine (H185) in PfDHODH seems to be the key for specificity over the human DHODH, as also shown for a previous group of PfDHODH inhibitors.¹⁸ Additionally, these results confirm that the most potent inhibitors reported here benefit from specific hydrophobic interaction with F188. The binding affinities of A77 1726 (**1**), **2**, and **3** were not affected by the F188A substitution (data not shown).

Conclusion

On the basis of an initial lead, a set of compounds was derived in which the members had a common hydrophilic portion linked to a variety of hydrophobic aromatic or heteroaromatic rings. From this series, compounds with nanomolar affinity for PfDHODH were identified that compete with ubiquinone for binding within the N-terminal channel. This mode of binding in the ubiquinone channel is supported by docking studies. The ligand/enzyme models predict that the inhibitors form H-bonds with amino acids (H185, R265, and Y528) in a similar manner to that observed for **1** binding in the PfDHODH crystal structure. Our mutagenesis studies further emphasize that H185 and R265 are involved in binding these inhibitors. It is interesting to note that similar mutagenesis studies on inhibitors identified by high-throughput screening also indicated a critical role for H185, whereas mutation of R265 had much less effect.¹⁸ Significantly, two of the most potent compounds identified in the current study were also shown to be the first PfDHODH inhibitors that inhibit the growth of cultured parasites at low micromolar levels. These results further highlight PfDHODH as a good target for antimalarial chemotherapeutics.

Experimental Section

General Methods. All solvents and reagents were used as purchased. Reactions were monitored by thin layer chromatography using aluminum-backed plates coated with silica gel (60 F₂₅₄ Merck), and purification of products by column chromatography was accomplished using standard silica gel 60 (200–400 mesh) obtained from a variety of suppliers. ¹H NMR spectra were recorded using a JEOL Lambda 400 spectrometer (referenced to CHCl₃), and mass spectra were recorded using a QP5050A Shimadzu GC/MS spectrometer. Elemental analysis was carried out using a Fisons EA 1108 CHN machine.

Inhibitors were prepared using the general procedure given below for compound **6**, unless otherwise stated. A similar method was applied to the synthesis of the other compounds, using diethyl ethoxymethylenemalonate in place of the acrylate where appropriate, giving yields of 40–60% (unoptimized). The yields were not adversely affected by use of excess acrylate or malonate (2–3 equiv), which could also be used as solvent in place of the toluene, except in the case of compound **7**, where further alkylation at the heterocyclic nitrogen was observed. If no precipitate formed on cooling to room temperature, then precipitation could be induced by cooling the reaction mixture to –20 °C for a period of several hours.

Synthesis. General Procedure: Synthesis of 2-Cyano-3-(9-ethyl-9H-carbazol-3-ylamino)acrylic Acid Ethyl Ester (6**).** A

mixture of 3-amino-9-ethylcarbazole (1.00 g, 4.8 mmol) and ethyl ethoxymethylenecyanoacrylate (1.04 g, 4.8 mmol), mixed with the aid of some toluene (5 mL), was heated slowly to 120 °C in an open flask over a period of 1–2 h. The reaction mixture was then cooled and filtered and the solid obtained was washed thoroughly with hexane to remove all the residual cyanoacrylate. Further purification using silica gel column chromatography with dichloromethane as eluent gave the title compound as a yellow-green crystalline solid (50%): mp 187–188 °C; ¹H NMR (CDCl₃, 400 MHz) δ 10.96 (1H, bd, *J* 13.7 Hz, =CH–NH), 8.07 (1H, d, *J* 7.8 Hz, ArH), 7.93 (1H, d, *J* 13.7 Hz, =CH–NH), 7.81 (1H, s, ArH), 7.52 (1H, t, *J* 8.2 Hz, ArH), 7.43 (1H, d, *J* 8.2 Hz, ArH), 7.40 (1H, d, *J* 8.6 Hz, ArH), 7.27 (1H, t, *J* 7.8 Hz, ArH), 7.21 (1H, d, *J* 8.6 Hz, ArH), 4.37 (2H, q, *J* 7.2 Hz, OCH₂ or NCH₂), 4.32 (2H, q, *J* 7.2 Hz, NCH₂ or OCH₂), 1.45 (3H, t, *J* 7.2 Hz, CH₂CH₃), 1.40 (3H, t, *J* 7.2 Hz, CH₂CH₃); MS (EI) *m/z* 333 (M⁺, 75), 287 (50), 272 (100). Anal. (C₂₀H₁₉N₃O₂) C, H, N.

N-(4-Bromo-2-methylphenyl)-2-naphthamide (2**).** 2-Naphthoyl chloride (1.0 g, 5.25 mmol) was dissolved in anhydrous DCM (25 mL). 4-Bromo-2-methylaniline (0.98 g, 5.25 mmol, 1.0 equiv) and triethylamine (1.10 mL, 7.87 mmol, 1.5 equiv) were added, and the reaction mixture was stirred at room temperature overnight. After this time, a solid precipitated out of solution and this was filtered and washed with several portions of DCM and water to give pure *N*-(4-bromo-2-methylphenyl)-2-naphthamide as a colorless microcrystalline solid (0.88 g, 2.59 mmol, 49%): mp 168–170 °C; ¹H NMR (300 MHz; CDCl₃) δ 8.38 (1H, bs, NH), 7.96–7.82 (6H, m, ArH), 7.63–7.54 (2H, m, ArH), 7.38–7.36 (2H, m, ArH), 2.34 (3H, s, CH₃); MS (ES⁺) *m/z* 340 (C₁₈H₁₄⁷⁹BrNO, MH⁺, 100), 342 (C₁₈H₁₄⁸¹BrNO, MH⁺, 100), 362 (C₁₈H₁₄⁷⁹BrNO, M⁺ + H₂O, 100), 364 (C₁₈H₁₄⁸¹BrNO, M⁺ + H₂O, 100); IR (solid, cm⁻¹) 3262, 3054, 1640, 1599, 1572. Anal. (C₁₈H₁₄BrNO) C, H, N.

N-(3,5-Dichlorophenyl)-2-methyl-3-nitrobenzamide (3**).** 2-Methyl-3-nitrobenzoic acid (1.0 g, 5.52 mmol) was added to neat thionyl chloride (20 mL, 0.28 mol, 50 equiv) at room temperature. The reaction mixture was heated at reflux for 2 h, followed by removal of the excess thionyl chloride by rotary evaporator. The acid chloride was then dissolved in anhydrous DCM (20 mL), 3,5-dichloroaniline (0.89 g, 5.52 mmol, 1.0 equiv) and triethylamine (1.20 mL, 8.28 mmol, 1.5 equiv) were added, and the reaction mixture was stirred at room temperature overnight. The mixture was then washed with 2 M NaOH (3 × 20 mL), 2 M HCl (3 × 20 mL), and brine (3 × 20 mL). The DCM layer was then dried (MgSO₄), filtered, and evaporated to leave crude product which was purified by silica gel flash chromatography (eluent 20% EtOAc–petroleum ether) and recrystallization from chloroform–hexane. *N*-(3,5-Dichlorophenyl)-2-methyl-3-nitrobenzamide was afforded as colorless needles (0.93 g, 2.87 mmol, 52%): mp 170–172 °C; ¹H NMR (300 MHz; CDCl₃) δ 7.91 (1H, d, *J* 7.9, ArH), 7.64 (1H, d, *J* 7.9, ArH), 7.59 (3H, bs, NH and 2 × ArH), 7.44 (1H, t, *J* 7.9, ArH), 7.19 (1H, s, ArH), 2.58 (3H, s, CH₃); MS (ES⁺) *m/z* 325 (C₁₄H₁₀³⁵Cl₂N₂O₃, M⁺, 50), 327 (C₁₄H₁₀³⁷Cl₂N₂O₃, M⁺, 30), 329 (C₁₄H₁₀³⁷Cl₂N₂O₃, M⁺, 5), 366 (C₁₄H₁₀³⁵Cl₂N₂O₃, M⁺ + MeCN, 100), 368 (C₁₄H₁₀³⁷Cl₂N₂O₃, M⁺ + MeCN, 60), 370 (C₁₄H₁₀³⁷Cl₂N₂O₃, M⁺ + MeCN, 10); HRMS (ES⁺, *m/z*) for C₁₄H₁₁³⁵Cl₂N₂O₃ calcd 325.0147, found 325.0151; IR (solid, cm⁻¹) 3279–3079, 1661, 1589, 1574, 1525.

Biological Assays. Protein Purification, Expression, and Analysis. Recombinant PfDHODH and HsDHODH truncated at the homologous location (amino acid residue 158 for PfDHODH and amino acid residue 30 for HsDHODH) were expressed in *E. coli* pyrD strain SØ6745 (kindly provided by K.F. Jensen) using a construct with a His-tag fusion as used in crystallographic studies (kindly provided by J. Clardy).^{5,7} These maintain the intact structure for the channel with both N-terminal α helices. After overnight incubation with 10 μM IPTG, cells were harvested and lysed by sonicating cell pellets in lysis buffer (50 mM NaH₂PO₄, 300 mM NaCl, 10 mM imidazole, adjusted to pH 8.0 with NaOH) containing 15 μL/mL protease inhibitor cocktail (Sigma-Aldrich), 1 mg/mL lysozyme (Sigma-Aldrich), and 2.5 mM DHO (Sigma-Aldrich), and the enzyme was purified by nickel agarose chromatography

(Qiagen). Enzyme purity was monitored by SDS-PAGE and concentration was determined spectrophotometrically using the Bradford protein assay (Bio-Rad).

Single amino acid substitutions were generated in the synthetic PfDHODH gene by introducing point mutations with the Quikchange PCR method (Stratagene). The following oligonucleotides were used for generating the amino acid substitutions (only the sense-strand primer shown): H185A, CGATGGTGAAATTTGCGCCGACCT-GTTTTGCTGCTTGG; F188A, GTGAAATTTGCCATGAC-TGGCCTTGCTGCTTGGGAAATATAAC; R265K, GCGAAAC-CGCGGATTTTAAGGACGTCAATCTCGC. Base substitutions were verified by DNA sequencing.

Acknowledgment. We are indebted to J. Clardy for his assistance and willingness in the sharing of reagents and data on the crystal structure of PfDHODH. Parasite cultivation was greatly aided by the technical expertise of M. Looker. Thanks are also due to R. Westwood and J. Coombes for helpful input in the early stages of the project. This work was supported in part by WHO Tropical Diseases Research Grant (to G.A.M.) and Medicines for Malaria Venture (to G.A.M.), Geneva, Switzerland. The authors thank the Wellcome Trust for a studentship to T.H. and the EPSRC for a studentship to M.D. The current address for A.M.W.S. is the School of Pharmacology, University of Puerto Rico, San Juan, PR.

Supporting Information Available: A table listing the degree of purity for all target compounds (area percent and retention time), a table listing the elemental analyses, details of the experimental procedures and spectroscopic data for each compound, and details of the biological assays. This material is available free of charge via the Internet at <http://pubs.acs.org>.

References

- Gardner, M. J.; Hall, N.; Fung, E.; White, O.; Berriman, M.; Hyman, R. W.; Carlton, J. M.; Pain, A.; Nelson, K. E.; Bowman, S.; Paulsen, I. T.; James, K.; Eisen, J. A.; Rutherford, K.; Salzberg, S. L.; Craig, A.; Kyes, S.; Chan, M. S.; Nene, V.; Shallom, S. J.; Suh, B.; Peterson, J.; Angiuoli, S.; Pertea, M.; Allen, J.; Selengut, J.; Haft, D.; Mather, M. W.; Vaidya, A. B.; Martin, D. M.; Fairlamb, A. H.; Fraunholz, M. J.; Roos, D. S.; Ralph, S. A.; McFadden, G. I.; Cummings, L. M.; Subramanian, G. M.; Mungall, C.; Venter, J. C.; Carucci, D. J.; Hoffman, S. L.; Newbold, C.; Davis, R. W.; Fraser, C. M.; Barrell, B. Genome sequence of the human malaria parasite *Plasmodium falciparum*. *Nature* **2002**, *419*, 498–511.
- Pink, R.; Hudson, A.; Mouries, M. A.; Bendig, M. Opportunities and challenges in antiparasitic drug discovery. *Nat. Rev. Drug Discovery* **2005**, *4*, 727–740.
- Tamta, H.; Mukhopadhyay, A. K. Biochemical targets for malaria chemotherapy. *CRIPS* **2003**, *4*, 6–9.
- Norager, S.; Jensen, K. F.; Bjornberg, O.; Larsen, S. *E. coli* dihydroorotate dehydrogenase reveals structural and functional distinctions between different classes of dihydroorotate dehydrogenases. *Structure* **2002**, *10*, 1211–23.
- Liu, S.; Neidhardt, E. A.; Grossman, T. H.; Ocain, T.; Clardy, J. Structures of human dihydroorotate dehydrogenase in complex with antiproliferative agents. *Structure* **2000**, *8*, 25–33.
- Hansen, M.; Le Nours, J.; Johansson, E.; Antal, T.; Ullrich, A.; Loffler, M.; Larsen, S. Inhibitor binding in a class 2 dihydroorotate dehydrogenase causes variations in the membrane-associated N-terminal domain. *Protein Sci.* **2004**, *13*, 1031–42.
- Hurt, D. E.; Widom, J.; Clardy, J. Structure of *Plasmodium falciparum* dihydroorotate dehydrogenase with a bound inhibitor. *Acta Crystallogr. D* **2006**, *62*, 312–323.
- Fox, R. I.; Herrmann, M. L.; Frangou, C. G.; Wahl, G. M.; Morris, R. E.; Strand, V.; Kirschbaum, B. J. Mechanism of action for leflunomide in rheumatoid arthritis. *Clin. Immunol.* **1999**, *93*, 198–208.
- Williamson, R. A.; Yea, C. M.; Robson, P. A.; Curnock, A. P.; Gadher, S.; Hambleton, A. B.; Woodward, K.; Bruneau, J. M.; Hambleton, P.; Spinella-Jaegle, S.; Morand, P.; Courtin, O.; Sautes, C.; Westwood, R.; Hercend, T.; Kuo, E. A.; Ruuth, E. Dihydroorotate dehydrogenase is a target for the biological effects of leflunomide. *Transplant. Proc.* **1996**, *28*, 3088–91.
- Copeland, R. A.; Marcinkeviciene, J.; Haque, T. S.; Kopcho, L. M.; Jiang, W.; Wang, K.; Ecret, L. D.; Sizemore, C.; Amsler, K. A.; Foster, L.; Tadesse, S.; Combs, A. P.; Stern, A. M.; Trainor, G. L.; Slee, A.; Rogers, M. J.; Hobbs, F. *Helicobacter pylori*-selective antibacterials based on inhibition of pyrimidine biosynthesis. *J. Biol. Chem.* **2000**, *275*, 33373–8.
- Marcinkeviciene, J.; Rogers, M. J.; Kopcho, L.; Jiang, W.; Wang, K.; Murphy, D. J.; Lippy, J.; Link, S.; Chung, T. D.; Hobbs, F.; Haque, T.; Trainor, G. L.; Slee, A.; Stern, A. M.; Copeland, R. A. Selective inhibition of bacterial dihydroorotate dehydrogenases by thiadiazolidinediones. *Biochem. Pharmacol.* **2000**, *60*, 339–42.
- Krungkrai, J. Purification, characterization and localization of mitochondrial dihydroorotate dehydrogenase in *Plasmodium falciparum*, human malaria parasite. *Biochim. Biophys. Acta* **1995**, *1243*, 351–60.
- McRobert, L.; McConkey, G. A. RNA interference (RNAi) inhibits growth of *Plasmodium falciparum*. *Mol. Biochem. Parasitol.* **2002**, *119*, 273–8.
- Baldwin, J.; Farajallah, A. M.; Malmquist, N. A.; Rathod, P. K.; Phillips, M. A. Malarial dihydroorotate dehydrogenase. Substrate and inhibitor specificity. *J. Biol. Chem.* **2000**, *277*, 41827–34.
- Kessl, J. J.; Lange, B. B.; Merbitz-Zahradnik, T.; Zwicker, K.; Hill, P.; Meunier, B.; Palsdottir, H.; Hunte, C.; Meshnick, S.; Trunpower, B. L. Molecular basis for atovaquone binding to the cytochrome bc₁ complex. *J. Biol. Chem.* **2003**, *278*, 31312–8.
- Hudson, A. T.; Dickins, M.; Ginger, C. D.; Gutteridge, W. E.; Holdich, T.; Hutchinson, D. B.; Pudney, M.; Randall, A. W.; Latter, V. S. 566C80: A potent broad spectrum anti-infective agent with activity against malaria and opportunistic infections in AIDS patients. *Drugs Exp. Clin. Res.* **2003**, *17*, 427–35.
- Heikkila, T.; Thirumalairajan, S.; Davies, M.; Parsons, M. R.; McConkey, A. G.; Fishwick, C. W.; Johnson, A. P. The first de novo designed inhibitors of *Plasmodium falciparum* dihydroorotate dehydrogenase. *Bioorg. Med. Chem. Lett.* **2006**, *16*, 88–92.
- Baldwin, J.; Michnoff, C. H.; Malmquist, N. A.; White, J.; Roth, M. G.; Rathod, P. K.; Phillips, M. A. High-throughput screening for potent and selective inhibitors of *Plasmodium falciparum* dihydroorotate dehydrogenase. *J. Biol. Chem.* **2005**, *280*, 21847–53.
- Shannon, P. V. R.; Eichholtz, T.; Linstead, D.; Masdin, P.; Skinner, R. Condensed heterocyclic compounds as anti-inflammatory and immunomodulatory agents. International patent number WO 99/45926, 1999.
- Boa, A. N.; Canavan, S. P.; Hirst, P. R.; Ramsey, C.; Stead, A. M. W.; McConkey, G. A. Synthesis of brequinar analogue inhibitors of malaria parasite dihydroorotate dehydrogenase. *Bioorg. Med. Chem.* **2005**, *13*, 1945–67.
- McLean, J. E.; Neidhardt, E. A.; Grossman, T. H.; Hedstrom, L. Multiple inhibitor analysis of the brequinar and leflunomide binding sites on human dihydroorotate dehydrogenase. *Biochemistry* **2001**, *40*, 2194–200.
- Knecht, W.; Henseling, J.; Loffler, M. Kinetics of inhibition of human and rat dihydroorotate dehydrogenase by atovaquone, lawsone derivatives, brequinar sodium and polyporic acid. *Chem. Biol. Interact.* **2001**, *124*, 61–76.
- Morris, G. M.; Goodsell, D. S.; Halliday, R. S.; Huey, R.; Hart, W. E.; Belew, R. K.; Olson, A. J. Automated docking using a Lamarckian genetic algorithm and empirical binding free energy function. *J. Comput. Chem.* **1998**, *19*, 1639–62.
- Zsoldos, Z.; Szabo, I.; Szabo, Z.; Johnson, A. P. Software tools for structure based rational drug design. *J. Mol. Struct.: THEOCHEM* **2003**, *666–667*, 659–65.
- Gillet, V. J.; Newell, W.; Mata, P.; Myatt, G.; Sike, S.; Zsoldos, Z.; Johnson, A. P. SPROUT: Recent developments in the de novo design of molecules. *J. Chem. Inf. Comput. Sci.* **1994**, *34*, 207–17.
- Wang, R.; Fu, Y.; Lai, L. A new atom-additive method for calculating partition coefficients. *J. Chem. Inf. Comput. Sci.* **1997**, *37*, 615–621.
- Copeland, R. A.; Davis, J. P.; Dowling, R. L.; Lombardo, D.; Murphy, K. B.; Patterson, T. A. Recombinant human dihydroorotate dehydrogenase: Expression, purification, and characterization of a catalytically functional truncated enzyme. *Arch. Biochem. Biophys.* **1995**, *323*, 79–86.
- Cheng, Y.; Prusoff, W. H. Relationship between the inhibition constant (K_i) and the concentration of inhibitor which causes 50 per cent inhibition (I₅₀) of an enzymatic reaction. *Biochem. Pharmacol.* **1973**, *22*, 3099–108.